

AUTOMATIC PIGMENT IDENTIFICATION ON ROMAN EGYPTIAN PAINTINGS BY USING SPARSE MODELING OF HYPERSPECTRAL IMAGES

Neda Rohani¹, Johanna Salvant², Sara Bahaadini¹, Oliver Cossairt¹, Marc Walton², Aggelos Katsaggelos¹

¹ Dpt. of Electrical Engineering and Computer Science, Northwestern University

² Center for Scientific Studies in the Arts (NU-ACCESS), Northwestern University

ABSTRACT

In this paper, we study the problem of automatic identification of pigments applied to paintings using hyperspectral reflectance data. Here, we cast the problem of pigment identification in a novel way by decomposing the spectrum into pure pigments. The pure pigment exemplars, chosen and prepared in our laboratory based on historic sources and archaeological examples, closely resemble the materials used to make ancient paintings. To validate our algorithm, we created a set of mock-up paintings in our laboratory consisting of a broad palette of mixtures of pure pigments. Our results clearly demonstrate more accurate estimation of pigment composition than purely distance-based methods such as spectral angle mapping (SAM) and spectral correlation mapping (SCM). In addition, we studied hyperspectral imagery acquired of a Roman-Egyptian portrait, excavated from the site of Tebtunis in the Fayum region of Egypt, and dated to about the 2nd century CE. Using ground truth information obtained using Raman spectroscopy, we show qualitatively that our method accurately detects pigment composition for the specific pigments hematite and indigo.

1. INTRODUCTION

The primary aim of identifying the pigments used on artworks is to characterize the palette of the artist, understand how these materials may change over time, to better inform conservation treatment of this invaluable cultural heritage, and to route out forgeries. More specifically, for the 2nd century AD Roman Egyptian portraits comprising this study (currently housed at the Phoebe A. Hearst Museum of Anthropology), these data not only help us to better understand the painting technology of this early period but also they are helping us to better characterize the global exchange and trade economy of the Roman era [1].

Reflectance spectroscopy and hyperspectral imaging are analytical methods that are becoming increasingly important for the documentation and characterizing works of art. Previous work in this area has employed a broad range of spectral information which relates the physical mineralogy of the pigment to its unique molecular spectral response. Hyperspectral imaging is inherently non-destructive and non-invasive and can be applied in-situ to recover reflectance curves on

a per pixel basis. Since each pigment has a characteristic reflectance response, these data can be interrogated using dictionaries of known spectra. These spectral dictionaries may either be physically modeled from the known molecular structure of the pigment mineralogy, learned directly from spectral samples of an artwork (e.g. learning so-called “endmembers” [2]), or they may be formed from previously collected spectra of representative pigment samples [3]. In this paper, we investigate the latter case, where ground truth measurements of a spectral library are provided. In particular, we form an over-complete dictionary that incorporates the inherent variability in the spectral response of a given pigment due to the non-uniformity in chemical compositions, paint thicknesses, pigment-binder ratios, sensor noise, and so on. We show quantitatively that such an over-complete dictionary representation produces more accurate estimation of pigment composition than using a dictionary consisting of a small set of pure endmembers alone.

Sparse modeling has been used in a diverse set of problems such as face recognition [4] and remote sensing [5]. In this paper, we cast pigment identification as an unmixing problem and solve it using sparse modeling. *To the best of our knowledge, we are the first to apply sparse modeling to the problem of pigment identification in paintings.* We build an over-complete dictionary from hyperspectral images of a reference pigment library composed of color swatches painted out on paper and canvas supports. These pigments were selected on the basis of what we already know about Roman painting from previous studies [6] and interrogating the portraits themselves using multi-analytical approach [7]. We then use our over-complete dictionary to decompose the measured test spectra of a pigment into a sparse coefficient vector using the ℓ_1 minimization solver [8]. The values in the sparse coefficient vector then directly correspond to abundances of pure pigments in the dictionary. We show that this approach produces quantitative performance advantages for estimating the composition of mixed pigments, and does so without the need for an explicit threshold selection strategy. To evaluate the performance of our algorithm, we applied our method to hyperspectral images captured from both our color swatch library and the mummy portrait itself. We compare our results with commonly used spectral angle mapping (SAM) and spectral correlation mapping (SCM) techniques and show that

our algorithm outperforms these methods. While we do not have exhaustive ground truth data for the pigment composition of the Fayum portrait, we compare against the ground truth pigment information of point samples measured using Raman spectroscopy. We also quantitatively evaluate the performance of our method using back-projection reconstruction error. Our method shows a significant improvement in both back-projection error and pigment decomposition relative to previous approaches.

2. PREVIOUS WORKS

Hyperspectral and multispectral data have already been used for pigment identification in previous studies such as [2], [3], [9], and [10]. Many of them [2], [3], [9], [10] can be seen as a method just based on nearest neighbor to classify pigments. They compare the unknown spectrum to the spectra of some reference spectra of pure pigments in a library. The whole procedure can be summarized in three steps: (i) making a spectral library (ii) defining a distance measure, (iii) assigning a label to an unknown pigment.

To build the spectral library, an endmember detection algorithm such as the pixel purity index algorithm [11] is usually used. These algorithms find the spectral signatures of the painting as pure pigments. However, they have important drawbacks. They usually need to know the number of endmembers beforehand [12]. Also, the obtained endmembers sometimes do not have any physical meanings. Once the endmembers are identified, the next step is to compare against the spectrum of a given pixel. A distance metric is used to assign the unknown pigment to the closest endmember in the library. To assign the label, a threshold value should be defined beforehand. For a given pixel, if the maximum similarity is higher than the threshold, the pixel is labeled as a member of the class with the smallest distance. Otherwise, the pixel is assigned as unlabeled (unknown). Such approaches suffer from some drawbacks. First, defining an appropriate distance function is not straightforward. Also, the value of the threshold is another crucial parameter. It has been shown that to detect different pigments in the hyperspectral paintings, sometimes more than one threshold value should be defined [10]. Lower threshold values are suitable for some pigments and to detect other pigments higher threshold values are used. Furthermore, the pixel is not labeled if its maximum spectral similarity is lower than the threshold. These metrics can be used for homogeneous areas and not highly mixed regions. In real paintings, there are numerous mixed pixels which are (non)linear combinations of two or more pigments.

In [10], a fully constrained spectral unmixing algorithm combined with linear mixing model [13] is applied to find the concentration of each endmember in each pixel. This work assumes that pigment spectra can be decomposed into a linear combination of endmembers from a known dictionary.

3. OUR APPROACH

3.1. Model Definition

We use sparse modeling to analyze pigment spectra. A sparse vector is a vector with only few non-zero elements. The sparse representation α of an unknown observation $\mathbf{y} \in \mathbb{R}^P$ with respect to a dictionary $\mathbf{D} \in \mathbb{R}^{P \times N}$, is the result of the constrained optimization problem:

$$\text{Minimize } \|\alpha\|_0 \text{ such that } \mathbf{y} = \mathbf{D}\alpha \quad (1)$$

where the ℓ_0 pseudo-norm counts the number of non-zero element in α . The problem in Eq. (3) can be solved by either involving greedy algorithms such as Matching Pursuit (MP) or Orthogonal Matching Pursuit (OMP) or by using relaxation techniques [14]. One such relaxation technique we adopt here is to replace the ℓ_0 norm with the ℓ_1 norm defined by:

$$\|\alpha\|_1 = \sum_{i=1}^N |\alpha_i| \quad (2)$$

where α_i is the i^{th} component of vector α . In our experiments, we use the SUNSAL (a LASSO solver) that has shown its efficiency for sparse unmixing for remote sensing [8]. It solves the constrained optimization problem:

$$\hat{\alpha} = \text{argmin}_{\alpha} \|y - \mathbf{D}\alpha\|_2^2 + \lambda \|\alpha\|_1 \text{ such that } \alpha \geq 0 \quad (3)$$

where λ controls the importance of the regularization term.

In this paper, we represent the unknown observation, i.e., the spectrum of a pigment, from a painting by \mathbf{y} . We estimate the sparse representation α corresponding to it by making a dictionary matrix \mathbf{D} and solving a convex optimization problem. Given \mathbf{D} and an unknown observation \mathbf{y} , we identify the constituent components of \mathbf{y} . In making our library or dictionary matrix \mathbf{D} , all the possible colors are considered and no further information about the number of pure pigments or their spectra is required. We assume that the spectrum of each pixel, i.e., observation, in the painting can be described as a linear combination of the atoms of the dictionary. Since each pixel in the real painting is composed of a small number of pigments compared to the total number of pigments in the composition as a whole, the obtained representation α should be a sparse vector.

3.2. Sparse Representation for Pigment Identification

Let us assume we have P spectral samples for each pigment. N sets of spectral samples are measured by capturing hyperspectral images of a library of pigments. We denote the number of pigments as K . From the measurements, we create K sub-dictionaries $\mathbf{D}_k \in \mathbb{R}^{P \times n_k}$, $k = 1, \dots, K$. Each sub-dictionary is formed as:

$$\mathbf{D}_k = [d_{k,1}, d_{k,2}, \dots, d_{k,n_k}] \quad (4)$$

where $d_{k,i}$ is the i -th spectrum of the k -th color and n_k is the number of the training samples for class k . Also, we define sub-coefficient vectors α_k corresponding to the coefficients of sub-dictionary \mathbf{D}_k as:

$$\alpha_k = [\alpha_{k,1}, \alpha_{k,2}, \dots, \alpha_{k,n_k}] \quad (5)$$

where $\alpha_{k,i}$ is the corresponding coefficient of $d_{k,i}$. The full dictionary or library \mathbf{D} is composed of all such sub-dictionaries, according to:

$$\mathbf{D} = [\mathbf{D}_1, \mathbf{D}_2, \dots, \mathbf{D}_K] \in \mathbb{R}^{P \times N} \quad (6)$$

The full coefficient vector α is composed of all such sub-coefficient vectors, according to:

$$\alpha = [\alpha_1, \alpha_2, \dots, \alpha_K] \in \mathbb{R}^{P \times N} \quad (7)$$

where $N = \sum_{k=1}^K n_k$ in Eq. (6) and (7).

Assuming a sample from a class can be estimated as a sparse linear combination of the training samples from that class, we can write

$$\mathbf{y}_k \approx \mathbf{D}_k \alpha_k = \alpha_{k,1} d_{k,1} + \dots + \alpha_{k,n_k} d_{k,n_k} \quad (8)$$

where \mathbf{y}_k is the observation or test sample from class k , $\alpha_{k,i}$ coefficients are defined as in Eq. (5), and $d_{k,i}$ atoms are defined as in Eq. (4). For any test sample, the non-zero components of α correspond to the concentration of each pigments present in the mixture.

3.3. Building the Pigment Dictionary

To form our dictionary \mathbf{D} , we use a set of pure commercial pigment exemplars, chosen and prepared as paint in our laboratory based on historic sources and archaeological examples, closely resembling the materials used to make ancient paintings. We captured the hyperspectral response of these pure exemplars and used these spectra to form a reference dictionary allowing us to study pigment identification via sparse regression. In addition, we used the samples from two online dictionaries: FORS Library and USGS Digital Spectral Library. To obtain a set of representative samples for each class and make the size of the dictionary reasonable, we apply the k-means clustering algorithm and use only the centroids of each cluster as atoms to populate the dictionary. Our final dictionary consists of $N = 406$ atoms and $K = 23$ unique pigments.

3.4. Pre-processing

Our captured spectra consist of 240 bands with $2nm$ resolution from 383 to 893nm. We observe that the low wavelength channels (20 bands) in the UV tend to be quite noisy, and are omitted. To reduce the effects of noise in the remaining bands, we average each four consecutive bands together, resulting in $P = 55$ channels in the each atom. The last step before solving the optimization problem is to normalize the atoms in the dictionary and test samples to have Euclidean norm equal to one.

3.5. Evaluation Measures

To evaluate the performance of our algorithm, we define a new coefficient vector, $\alpha' \in \mathbb{R}^K$ with elements:

$$\alpha'_k = \sum_{j=1}^{n_k} \alpha_{k,j} \quad \text{for } k \in 1, \dots, K \quad (9)$$

where α'_k is the k^{th} components of vector α' , and $\alpha_{k,j}$ is the

j^{th} components of vector α_k . The new coefficient vector α' is simply the sum of the coefficients for the atoms corresponding to each pigment. Unfortunately, in our experiments we do not have access to ground truth information on the concentration of pigments in the spectra we measured. Instead, we use reconstruction error as a metric of evaluation.

4. EXPERIMENTS

To evaluate the performance of our algorithm, we organize two sets of experiments. To compare our results with previous methods for pigment identification, we use SAM, SCM and linear unmixing [13]. In this section, we refer to our algorithm as the sparse unmixing method. In the linear unmixing algorithm, we refer to the atoms of the dictionary as endmembers.

4.1. Real Pigment Mixtures

In our first experiment, we use seven pure pigments: "gypsum, calcite, indigo, lead white, Egyptian blue, goethite and hematite". We create 17 mixtures of these pigments by mixing two/three together and painting onto a color swatch. We then capture a hyperspectral image of each color swatch and use our sparse unmixing method to estimate the sparse coefficients for each measured spectral sample. In this experiment, we have partial ground truth information in the form of the label of each pigment used in each mixture but we do not have direct access to the true coefficient values (i.e. pigment concentration). Table 1 shows the composition of each mixture. We compare the performance of the two unmixing algorithms (sparse vs. linear) by reporting the average reconstruction error. Our algorithm produces less reconstruction error for each of the 17 mixtures in our experiment, significantly less for a number of samples.

We analyze the results of four algorithms (SAM, SCM, linear and sparse unmixing) on mixture 6 which is composed of two pure pigments: indigo and hematite. The average spectra of seven pure pigments are shown in Fig. 1 (a). For reference, the average spectrum of the mixture with that of its pure pigments, (indigo, hematite and mixture) are shown in Fig. 1 (b). As it can be observed, the average spectrum of the mixture is very similar to the average spectrum of the indigo curve shown in the figure, indicating a greater concentration of indigo than hematite. We calculate the spectral angle and spectral correlation similarities of each pixel in the mixture with the endmembers in the dictionary. We also apply the linear and sparse unmixing algorithms to estimate the coefficients of each pixel of the mixture. To compare the results of four algorithms, we take the average of the similarity coefficients of all pixels of the mixture for seven colors. In Fig. 1 (c), the numbers on the horizontal axis refer to the pigment in our pure pigment list. The vertical axis shows the average similarity coefficient obtained by each algorithm for each color. As it can be observed in the figure, with both unmixing algorithms, the estimated coefficients for the first two colors (gypsum and calcite) are very small ($< 10^{-4}$). However, linear unmixing estimates goethite (color 6) to be greater than

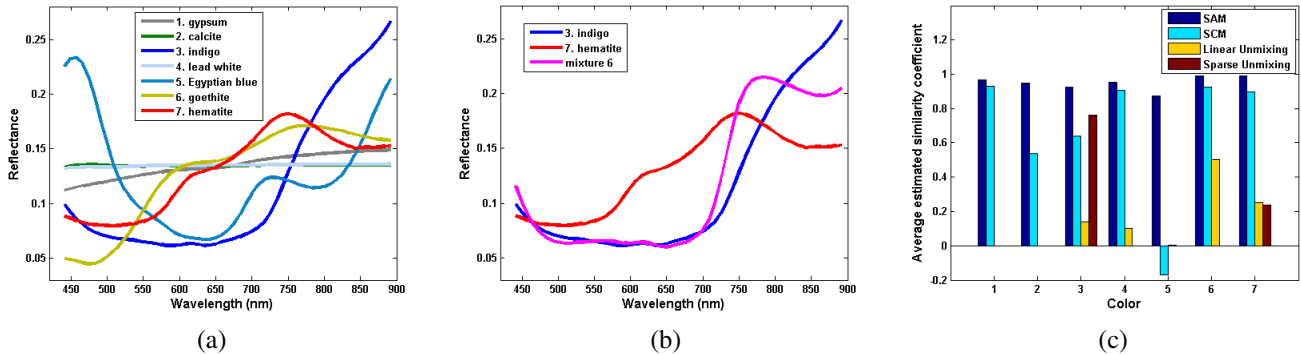


Fig. 1: (a) Endmembers spectra, (b) Average spectra of indigo, hematite and the mixture, (c) Comparison of the estimated similarity coefficient of four algorithms. Only our spectral unmixing algorithm correctly estimates that the sole pigments in the mixture are hematite and indigo.

Table 1: Average reconstruction error For 17 mixtures (our algorithm vs. linear unmixing)

Mixture	Our Alg.	Linear Unmix.
gypsum+lead white	0.010	0.011
calcite+goethite	0.045	0.081
calcite+hematite	0.038	0.096
calcite+lead white	0.056	0.125
indigo+lead white	0.053	0.112
indigo+hematite	0.013	3.226
indigo+goethite	0.010	0.011
hematite+lead white+goethite	0.045	0.081
Egyptian blue+lead white+goethite	0.038	0.096
Egyptian blue+hematite+goethite	0.056	0.125
Egyptian blue+hematite+lead white	0.053	0.112
hematite+goethite	0.013	3.226
hematite+Egyptian blue	0.010	0.011
hematite+lead white	0.045	0.081
Egyptian blue+lead white	0.038	0.096
goethite+lead white	0.056	0.125
goethite+Egyptian blue	0.053	0.112

indigo (color 3) and hematite (color 7). As discussed previously, SAM and SCM are not suitable to determine pigment concentration in highly mixed regions. By studying the SAM result in Fig. 1 (c), it is unclear how to choose the proper threshold to identify the constituent pigments in the mixture. The most similar pigments to the mixture pixels appear to be goethite, hematite and gypsum. Using SCM, the most similar pigments are goethite, gypsum and lead white. Only our spectral unmixing algorithm correctly estimates that the sole pigments in the mixture are hematite and indigo.

In our second experiment, we applied our method to a Roman-Egyptian portrait, excavated from the site of Tebtunis in the Fayum region of Egypt. For this painting, ground truth measurements of pigment composition at a small set of point

locations were measured using Raman spectroscopy. In Fig. 2 (a), the studied portrait is shown. The red arrows indicate the pixels for which ground truth information has indicated the presence of either hematite or indigo. As can be observed in Fig. 2 (b), our method correctly estimates the presence of indigo in the lozenge of the crown and clavus regions, which is confirmed by our analysis via Raman. In Fig. 2 (c), we observe that hematite is used more in the face region, which is also confirmed by our ground truth measurements.

5. CONCLUSION AND FUTURE WORKS

In this paper, we introduced the first application of sparse unmixing to the problem of pigment identification. This method addresses several limitation of previous methods applied to the pigment identification problem. We showed that distance based methods such as SAM and SCM do not work well in scenarios with highly mixed regions and that our sparse unmixing algorithm can estimate the pigment composition more accurately than a linear unmixing method.

As part of our future work, we will further study the mixing model of the pigments to improve our modeling. We will also investigate feature selection methods to choose more meaningful representations of our pigment spectra. For real data, we will explore super pixel representations to merge spectrally similar neighboring pixels. This new representation will reduce the number of test samples and also the effects of noise and artifacts. We will also apply dictionary learning based methods to build a richer reference spectra library.

6. ACKNOWLEDGMENTS

This collaborative initiative is part of NU-ACCESSs broad portfolio of activities, made possible by generous support of the Andrew W. Mellon Foundation as well as supplemental support provided by the Materials Research Center, the Office of the Vice President for Research, the McCormick School of Engineering and Applied Science, and the Department of Materials Science and Engineering at Northwestern University. This work was funded in part by NSF CAREER grant

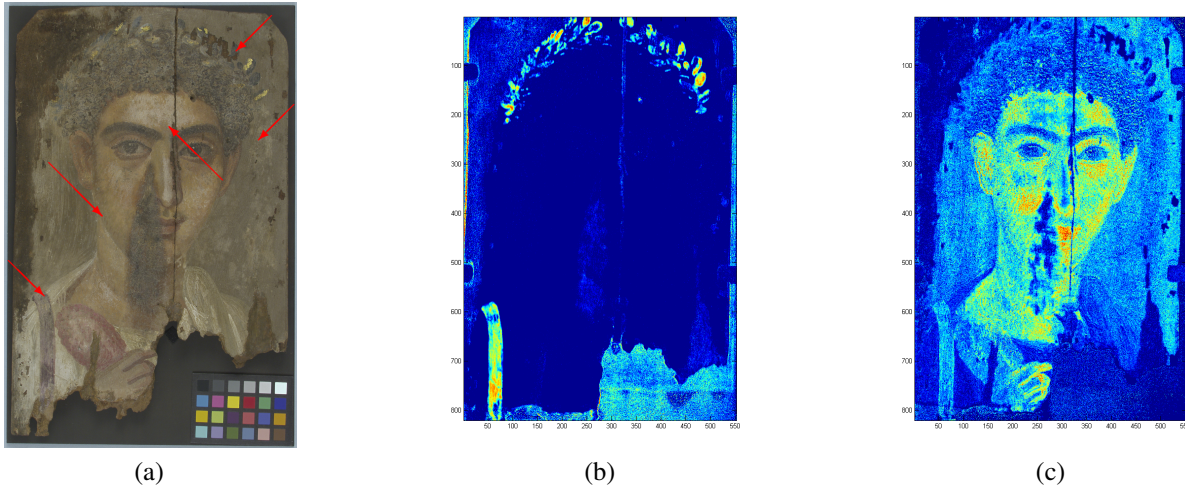


Fig. 2: (a) Studied Portrait (arrows point to locations where ground truth pigment composition is known), (b) Coefficient map of indigo, (c) Coefficient map of hematite. Our sparse unmixing algorithm correctly estimates pigment composition in the select areas where ground truth information is known.

IIS-1453192. We are grateful to Jane Williams, Conservator at the Phoebe A. Hearst Museum of Anthropology, for granting us access to the portrait. We wish to thank Noalle Fellah for preparing samples and model paintings during her Oberlin College winter term placement at NU-ACCESS. Also Valentine Talland, Senior Objects Conservator, Isabella Stewart Gardner Museum, for supplying pigment swatches scanned in the course of this study.

References

- [1] M. S. Walton and K. Trentelman, "Romano-egyptian red lead pigment: A subsidiary commodity of spanish silver mining and refinement," *Archaeometry*, vol. 51, no. 5, pp. 845–860, 2008.
- [2] J. K. Delaney, J. G. Zeibel, M. Thoury, and et. al, "Visible and infrared imaging spectroscopy of picasso's harlequin musician: mapping and identification of artist materials in situ," *Applied spectroscopy*, vol. 64, no. 6, pp. 584–594, 2010.
- [3] P. Almeida, C. Montagner, R. Jesus, and et. al, "Analysis of paintings using multi-sensor data," in *Signal Processing Conference, 2013 Proceedings of the 21st European. IEEE*, 2013, pp. 1–5.
- [4] J. Wright, A. Y. Yang, A. Ganesh, and et. al, "Robust face recognition via sparse representation," *Pattern Analysis and Machine Intelligence, IEEE Transactions on*, vol. 31, no. 2, pp. 210–227, 2009.
- [5] M. Iordache, J. M. Bioucas-Dias, and A. Plaza, "Sparse unmixing of hyperspectral data," *Geoscience and Remote Sensing, IEEE Transactions on*, vol. 49, no. 6, pp. 2014–2039, 2011.
- [6] C. Rozeik, J. Dawson, and M. Wright., "Decorated surfaces on ancient egyptian objects: Technology, deterioration and conservation," *Archetype*, 2010.
- [7] M. Ganio, J. Salvant, J. Williams, and et. al, "Investigating the use of egyptian blue in roman egyptian portraits and panels from tebtunis, egypt," *Applied Physics A*, vol. 121, no. 3, pp. 813–821, 2015.
- [8] J. M. Bioucas-Dias and M. A. Figueiredo, "Alternating direction algorithms for constrained sparse regression: Application to hyperspectral unmixing," in *Hyperspectral Image and Signal Processing: Evolution in Remote Sensing, 2010 2nd Workshop on. IEEE*, 2010, pp. 1–4.
- [9] A. Pelagotti, A. D. Mastio, A. D. Rosa, and A. Piva, "Multispectral imaging of paintings," *Signal Processing Magazine, IEEE*, vol. 25, no. 4, pp. 27–36, 2008.
- [10] H. Deborah, S. George, and J. Y. Hardeberg, "Pigment mapping of the scream (1893) based on hyperspectral imaging," in *Image and Signal Processing*, pp. 247–256. Springer, 2014.
- [11] F. Chaudhry, C. Wu, W. Liu, and et. al, "Pixel purity index-based algorithms for endmember extraction from hyperspectral imagery," *Recent Advances in Hyperspectral Signal and Image Processing*, vol. 37, no. 2, pp. 29–62, 2006.
- [12] O. Eches, N. Dobigeon, and J. Tourneret, "Estimating the number of endmembers in hyperspectral images using the normal compositional model and a hierarchical bayesian algorithm," *Selected Topics in Signal Processing, IEEE Journal of*, vol. 4, no. 3, pp. 582–591, 2010.
- [13] D. C. Heinz and C. Chang, "Fully constrained least squares linear spectral mixture analysis method for material quantification in hyperspectral imagery," *Geoscience and Remote Sensing, IEEE transactions on*, vol. 39, no. 3, pp. 529–545, 2001.
- [14] M. Elad, *Sparse and Redundant Representations: From Theory to Applications in Signal and Image Processing*, Springer New York, 2010.